Materials Research. 2017; 20(Suppl. 1): 96-103
DOI: http://dx.doi.org/10.1590/1980-5373-MR-2017-0406
© 2017

Production of TiO_2 Coated Multiwall Carbon Nanotubes by the Sol-Gel Technique

Laura Angélica Ardila Rodríguez*[a]*, Matheus Pianassola[a], Dilermando Nagle Travessa[a]

[a]Universidade Federal de São Paulo (UNIFESP), Instituto de Ciência e Tecnologia, Laboratório de Metais e Processamentos Avançados, São José dos Campos, SP, Brazil

Received: April 26, 2017; Revised: October 01, 2017; Accepted: November 10, 2017

In recent years, efforts in developing high strength-low density materials are increasing significantly. One of the promising materials to attend this demand is the carbon nanotube (CNT), to be used mainly as a reinforcing phase in lightweight metal matrix composites (MMC). In the present work, the sol-gel technique has been employed to obtain TiO_2 coating on the surface of commercial multiwall carbon nanotubes (MWCNT). The aim of such coating is to improve the thermal stability of MWCNT in oxidize environment, which is necessary in most of MMC processing routes. Calcination in inert atmosphere was performed in order to crystallize a stable coating phase. The hybrid CNT/TiO_2 nanocomposite was characterized by X-Ray Diffractometry (XRD), Raman spectroscopy, Thermogravimetry (TGA) and Field Emission Gun - Scanning Electron Microscopy (FEG-SEM). The coating structure was observed to change from anatase to rutile, as the calcination temperature increases from 500 to 1000ºC. Results from thermogravimetric analysis showed that the samples calcined at 1000 ºC were more resistant to oxidation at high temperatures.

Keywords: *Carbon nanotubes, TiO_2, sol-gel, surface coating.*

1. Introduction

In the last three decades, since the carbon nanotubes (CNT) were discovered, intense research efforts have been done in order to exploit their excellent mechanical properties. Particularly a Young modulus and a tensile strength of around 1 TPa[1,2] and 200 GPa[3], respectively, made CNT highly prone to act as a reinforcement phase in several types of composite materials, including polymeric, ceramic and metal matrix.

Metal matrix composite materials (MMC) have being studied due to their potential produce lightweight structures for the transportation industry, mainly automotive, aeronautical and space[4]. The use of CNT as reinforcing phase for MMC has been a challenge because of its high surface area and the resulting Van der Walls interactions that make difficult its dispersion[5,6]. Furthermore, it has been observed that CNT has low wettability by most metals, resulting in low interaction with the matrix and low potential for strengthening by load transfer mechanisms[7-9].

Many authors have tried to improve CNT dispersion in metal matrix by several processing routes, as thermal spray[6,10], high energy ball milling[11], friction stir processing[12]. In most cases, it has been observed that the extreme processing conditions mainly related to high temperatures and stresses can damage the CNT structure[13,14]. CNTs are thermodynamically stable up to 2200 ºC if no oxygen or other reactive impurities are present. However, they are quite reactive with oxygen at temperatures above 500ºC, forming carbon oxide or dioxide[15]. Consequently, high temperature composite processing can lead to CNT to degrade if oxygen or reactive elements are present. Some advanced MMCs processing routes, like spark plasma sintering[16,17], involves inert gas fluxes or vacuum that can preserve the CNT integrity. However, such processing routes are usually expensive, requiring costly equipment and gases. Furthermore, such processes are not suitable for high productivity.

Conventional processes capable of achieving high productivity, such as hot extrusion or hot rolling[18,19], are normally performed without gas protection. Other industrial scale processes like plasma spray, used for parts surface protection or repair, involve temperatures higher than the graphite boiling point (4900 ºC). Consequently sublimation of carbon nanotubes during the plasma spray forming[20] can occur. Alternatively, in the High Velocity Oxy-Fuel (HVOF) process, temperatures are lower than plasma spray, but in this case, CNTs are in close contact with the working gas, reacting with the containing oxygen[21]. Therefore, a large amount of the CNTs embedded in the molten Al can be lost during HVOF spraying.

Aluminum can also react with the carbon nanotubes during the production of Al/CNT composites, even under protective atmospheres [7,22]. This reaction is concentrated at CNT surface defects and forms aluminum carbide (Al_4C_3). Depending on the processing conditions, this reaction can extend to few angstroms at the metal/CNT interface or, under extreme conditions as in processes involving liquid Al, it can totally consume the CNTs[23]. Ci et. al [7]reported that the formation of Al_4C_3 at the interface can improve the interfacial bonding to some extension. However, the Al_4C_3 is easily decomposed in $Al(OH)_3$, CO_2 and H_2 in presence

*e-mail: laardilar88@gmail.com

of liquid water or moisture. Park et al[24] found that Al_4C_3 can decompose in less than 120 h, when exposed to a wet environment, resulting in matrix to CNT interface debonding that accelerates the fatigue crack growth rates on Al/SiC composites tested in moisture environment.

In order to mitigate much of the difficulties in obtaining CNT reinforced MMC, in the present work, we propose to coat the CNT with a ceramic material [25,26], expecting to improve their adherence with the metallic matrix, to make easier their dispersion during the composite processing and to protect the CNT from severe processing conditions and from excessive reaction with the matrix[27]. As a result, the unique characteristics of CNT those make them very interesting as reinforcing phase in MMC can be fully exploited.

Manivannan et al[25] employed the sol gel method in order to coat MWCNT with zirconia, and the resulting MWCNT/ZrO_2 composite was sintered in nitrogen atmosphere at different temperatures in order improve their bonding at the interface. They observed from TGA studies that oxidation resistance of the sintered composite was improved with proper selection of sintering temperature. Inam et al [26] found that fabricating alumina-CNT nanocomposite by atomic layer deposition (ALD) resulted in encapsulated nanotubes that provided a shielding effect against further oxidation during the composite consolidation by spark plasma sintering. The thicker alumina coating obtained by ALD, the better the CNT resistance to oxidation during subsequent sintering. Jo et al [27] coated carbon nanofibers (CNFs) with titanium dioxide by the sol gel method, in order to improve their wettability and prevent reactions with molten aluminum matrix during the production of Al/CNF by liquid pressing process. The authors found from TGA analysis that TiO_2 coated CNFs could maintained their mass up to 1000ºC in the air atmosphere without significant losses, confirming that a TiO_2 coating can enhance the structural stability of CNFs in severe environments, preventing the Al_4C_3 formation.

Within the context of the protection of carbon nanotubes during the production of metal/CNT composites, in the present work we describe the synthesis of a TiO_2 coating formed on the surface of multiwall carbon nanotubes (MWCNT) by the sol-gel route, using titanium tetra isopropoxide (TTIP) as a precursor. Processing parameters such as TTIP: H_2O molar ratio in the solution and MWCNT concentration are investigated and related to the quality of the obtained coating. The structure and morphology of the hybrid MWCNT/TiO_2 were investigated by X-ray diffraction (XRD), field emission gun-scanning electron microscopy (FEG-SEM), Raman spectroscopy and thermogravimetric analysis (TGA).

2. Experimental

2.1. Materials

In this study Baytubes® C 150 P MWCNT, were used. The MWCNT were produced by Bayer Materials Science-Germany by the CVD process, resulting in a minimum purity level of 95%, internal and external diameters of the order of 4 and 13 nm, respectively, and length greater than 1 µm. Nitric acid 65% PA, sulfuric acid PA-ACS analytical grade, Sodium dodecyl sulphate (Synth), Ethanol 99.8% P.A, Titanium tetra isopropoxide (Aldrich), glacial acetic acid 99.8% (Neon) and Ammonium hydroxide PA (Synth) were the reagents used to functionalize and coat the MWCNT.

2.2. Carbon nanotubes functionalization

Aiming to introduce surface functional groups on the MWCNT surface that are necessary to anchor the TiO_2 layer, the MWCNT were acid treated in 60 mL of 1: 3 (v:v) of nitric acid and sulfuric acid for 6 hours under magnetic stirring. The resulting mixture was washed in deionized water and dried at 80 º C for 15 hours.

2.3. MWCNT/TiO_2 nanocomposite synthesis

TiO_2 coated MWCNTs were obtained by the sol-gel method using titanium tetra isopropoxide (TTIP) as precursor. One of the problems of the sol gel technique is that it normally leads to a non-uniform coating, resulting simultaneously in some uncoated surface regions along with excessive deposits in other regions of the MWCNT surface [28]. In the present work, it was employed the Gao et.al [29] method, with modifications. The use of surfactants as sodium dodecyl sulphate (SDS) significantly improved the dispersion of MWCNTs in aqueous solution, providing an efficient support to the TiO_2 nanoparticles to growth and attach to the MWCNTs surface via noncovalent bond.

Initially, a constant mass of MWCNT was dispersed in Milli-Q water, with 2% wt. of sodium dodecyl sulphate (SDS) and sonicated for 30 min. Then 20 mL of ethanol was added to the mixture and stirred for another 30 min, forming a MWCNT suspension. In parallel, titanium tetra isopropoxide (TTIP) was mixed with 15 mL of ethanol and glacial acetic acid under stirring for 30 min, forming the TiO_2 solution. Finally, the TiO_2 solution was added dropwise in the MWCNT suspension under vigorous stirring that was kept for 2 hours in order to complete the reaction. At this stage, the TTIP precursor hydrolyses in contact with the water present in the MWCNT suspension. The resulting TTIP:H_2O molar ratios were 1:60, 1:220 and 1:340, and the weight ratio of MWCNT related to the TiO_2 formed was 28%. Ammonium hydroxide was added dropwise until a pH of 9 was reached, and finally 10 mL of ethanol were added to the mixture, keeping the stirring for another 30 min. The final suspension was centrifugated and washed three times in ethanol. The drying process was carried out for 15 hours at 60º C in order to obtain the powdered TiO_2-coated MWCNT.

For comparison purpose, the same procedure was performed for a TTIP:H_2O molar ratio of 1:220 and varying the amount of MWCNT, resulting in two additional MWCNT to TiO_2 weight ratios: 16% wt. and 23% wt. Table 1 resumes the relative quantities of MWCNT, TTIP and H_2O employed.

Table 1. Relative proportion of MWCNT, TTIP and H_2O used to produce TiO_2-coated MWCNT.

MWCNT % wt.[1]	TTIP: H_2O molar ratio
28	1:60
28	1:340
28	1:220
23	1:220
16	1:220

[1]percent of MWCNT, related to the total weight of the MWCNT/TiO_2 hybrid

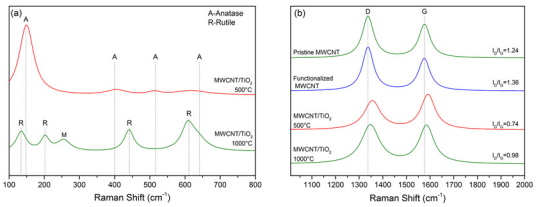

Figure 1. Raman Spectra in the range of: (a) 100-800 cm^{-1} from TiO_2 coated MWCNT calcined at 500 and 1000ºC; (b) 1000-2000 cm^{-1} from pristine, functionalized MWCNT and TiO_2 coated MWCNT calcined at 500 and 1000ºC.

The hybrid MWCNT/TiO_2 obtained was calcined at temperatures of 500 and 1000º C for 3 hours in an inert argon atmosphere, in order to crystallize the amorphous coating layer obtained from the sol-gel process.

2.4 Samples characterization

The TiO_2-coated MWCNT were characterized by X-ray diffraction, in order to verify the crystallinity degree of the obtained coating. A Rigaku X-ray diffractometer model Ultima IV was used, operating with Cu Kα radiation (λ = 1.54178 Å) with a voltage of 40kV and 30mA of current. Multiple detectors (fast detection mode) were used at steps of 0,01º and a speed of 5º/min, resulting in a high signal level. The microstructure was analyzed using a Tescan model Mira 3 field emission gun-scanning electron microscope (FEG-SEM). The SEM images were formed from Secondary Electrons (SE), at 2 mm of work distance and 5kV. Raman spectroscopy was recorded by a Horiba LabRAM microscope with 514 nm laser. The Raman spectra were collected using 3 accumulations in 30 seconds, in the range of 50 to 2000 cm^{-1}. Thermal gravimetric analyzes were performed on a NETZSCH STA 449 F1 Jupiter equipment (TG-DSC / DTA) with a heating rate of 10º C / min, between 50 and 1000º C in O_2 atmosphere with a flow of 20 mL / min.

3. Results and Discussion

Figure 1(a) presents the Raman spectra for the hybrid MWCNT/TiO_2, after calcination at temperatures of 500 (a) and 1000ºC (b). As the MWCNT are coated by the TiO_2 layer, a number of scattering bands form in the Raman spectra besides the D and G bands: Eg (142 cm^{-1}), B1g (399 cm^{-1}), A1g (518 cm^{-1}), and Eg (641 cm^{-1}) bands from TiO_2 anatase structure are present in the sample calcined at 500º C. The Raman spectra changes for samples calcined at 1000ºC. Bands of A1g (612 cm^{-1}) and Eg (446 cm^{-1}), as well as from multi-photon scattering process (230 cm^{-1},"M" in the Figure 1(a)) from TiO_2 rutile structure [30] are present. These results show that the TiO_2 structure changes from anatase to a more stable rutile structure as the calcination temperature increases.

The Figure 1 (b) shows the Raman spectra in the range of the main carbon scatters, for pristine and functionalized MWCNT, as well as for the calcined TiO_2 coated MWCNT. It is known that the intensity of the bands D and G are associated respectively to structural disorder and to the graphitic nature of the MWCNT, related to the tangential stretching mode of the C=C bond[31,32]. The ratio between the intensities of D and G bands (I_D/I_G ratio) is expected to increase after the MWCNT functionalization, as surface defects are created in the nanotubes. As expected, the I_D/I_G ratio increases from 1.24 to 1.36, after acid functionalization. After calcination at 500ºC (c), the I_D/I_G ratio was found to decrease to 0.74. This behavior can be attributed to the thermal induced rearrangement of the carbon structure [33], and consequently, it would be expected that calcination at higher temperatures would continuously decrease the I_D/I_G ratio. However, an opposite effect was observed. After calcination at 1000ºC, the measured I_D/I_G ratio was 0.98. Anatase to rutile phase transformation is supposed to be responsible for this behavior. Such phase transformation reconstructive, requiring the rearrangement of the Ti-O atoms to fit to the new structure. Furthermore, significant grain growth and densification (reduction in specific surface area) are expected [34] when anatase transform to rutile structure. As Ti-O atoms are tightly bonded to the MWCNT surface, stresses associated to the TiO_2 reconstruction should be transferred to the nanotubes, increasing the MWCNT network distortion and consequently the intensity of the D scatter band.

The D and G bands of pristine MWCNT were identified at 1337.37 and 1576.31 cm^{-1}, respectively. After acid functionalization, these bands were found to slightly shift to 1337.33 cm^{-1} and 1576.22 cm^{-1}, respectively. In the TiO_2 coated nanotubes, calcined 500 and 1000ºC, these bands are considerably shifted to higher wave numbers, between 1342-1359 cm^{-1} and 1583-1594 cm^{-1}, respectively. In this case, the upshift of the D band is related to stress induced by the TiO_2 bonded to the surface of the MWCNT [35,36] and the upshift in the G band is due to the high interaction level between the TiO_2 and the MWCNT [37,38].

Figure 2 shows the X-ray diffractograms obtained from samples of TiO_2 coated MWCNT, calcined at 500

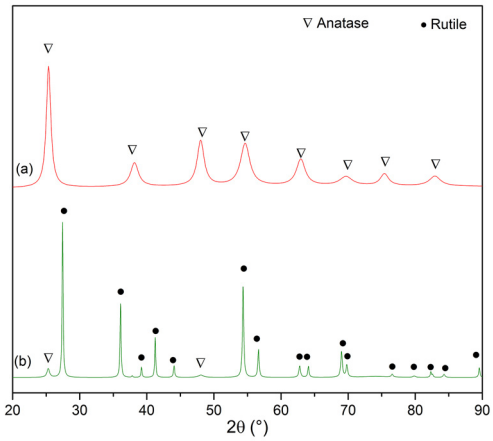

Figure 2. XRD patterns of TiO_2 coated MWCNT, synthetized by the sol-gel process and calcined at (a) 500ºC and (b) 1000ºC.

and 1000ºC. The formation of the TiO_2 phase is confirmed, having two different structures depending on the calcination temperature. At 500ºC the diffraction peaks correspond to the Anatase structure (JCPDS Nº 21-1272), as observed in Figure 2A. The sample calcined at 1000ºC exhibited peaks predominantly from the Rutile phase (JCPDS Nº 21-1276), see Figure 2B, along with a small amount of Anatase indicated by the presence of its main diffraction peak (101) at 2θ = 25.28º. From the equation (1), the weight percent of the Anatase phase, W_A, was estimated to be 4.9%.

$$W_A = \frac{100}{1 + 1.265\, I_R/I_A} \qquad (1)$$

In equation (1), I_A denotes the intensity of strongest Anatase reflection, (101; 2θ=25.28º.) and I_R is the intensity of strongest rutile reflection (110; 2θ=27.44º)[39,40].

A rough approximation of the crystallite size of the samples was calculated by the well-known Scherrer's equation (2)[41] based on the full width at half maximum (FWHM), denoted as B in the equation, where θ is the diffraction angle and λ is the X-ray wavelength corresponding to CuK_α radiation.

$$D = \frac{0.9\lambda}{B\cos\theta} \qquad (2)$$

The obtained crystallite sizes were 10±2 nm for the (101) Anatase peak, in the sample calcined 500ºC, and 27±3 nm for the rutile peak (110), in the sample calcined at 1000ºC. The Cu $k\alpha_2$ contribution was not removed before measuring the FWHM. These results show that the Anatase to Rutile transformation is accompanied by grain growth, as expected [34].

The morphological aspect of the TiO_2 coated MWCNT was observed by FEG-SEM. The Figure 3 shows the morphology of the as supplied MWCNT. Although they are highly agglomerated, it is possible to note their high aspect ratio. It can also be observed in Figure 3(a) the presence of metallic nanoimpurities at the extremities of few nanotubes, corresponding to the remaining seeds from the MWCNT synthesis process. After acid functionalization, these impurities are dissolved, as observed in Figure 3(b). It is also observed from Figure 3(b) that the individual nanotubes are clearly visible after acid functionalization, being easier to differentiate from one to another. It is expected that acid functionalization also dissolve eventual amorphous regions present in the MWCNT[42,43].

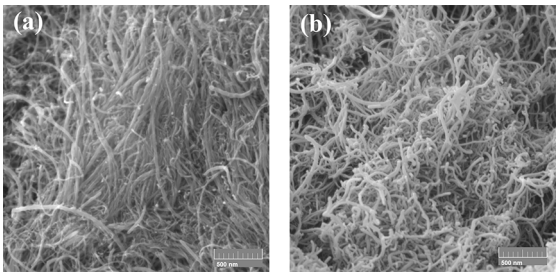

Figure 3. FEG-SEM images of (a) Pristine MWCNT and (b) Functionalized MWCNT.

Samples of TiO_2-coated MWCNT, obtained after the sol-gel process using different titanium isopropoxide (TTIP) to H_2O molar ratios, are shown in Figure 4. In Figure 4(a), the molar ratio of 1:60 resulted in still entangled MWCNT, surrounded by agglomerates of the synthetized TiO_2 particles. This is a consequence of the low quantity of the water used to prepare the MWCNT suspension. The concentration of MWCNT in the suspension was very high (13.5 mg/ml), making difficult their fully dispersion. In the other extreme, decreasing the TTIP to H_2O molar ratio to 1:340 significantly improved the MWCNT dispersion, as observed in Figure 4(c). However, the volume of TiO_2 particles formed is very high. In this case, the concentration of MWCNT related to water was very low (1 mg/ml), promoting a quick growth of TiO_2 nanoparticles since the hydrolysis process is very fast and under this condition, the formation of isolated TiO_2 nanoparticles in the solution is preferential over their growth as a layer over the MWCNT surface.

When the TTIP:H_2O molar ratio was set at an intermediate value of 1:220, it is apparent that a thin and very homogenous coating layer of TiO_2 was formed over the MWCNT surface, see the Figure 4(b). Very few isolated TiO_2 nanoparticles are formed. In this case, the MWCNT concentration in the suspension (8 mg/ml) results in an optimized balance between their dispersion and a moderate hydrolysis rate that is responsible for a controlled growth of the TiO_2 coating layer over the nanotubes surface.

As the best TTIP:H_2O molar ratio was found to be 1:220 (see Figures 4(a) to 4(c)), the following step was to improve the homogeneity of the coating layer formed, by adjusting the MWCNT to TiO_2 weight ratio. It can be observed from Figures 4(d) to 4(f) that the MWCNT was successfully and homogenously coated by different thicknesses of TiO_2. In the Figure 4(d), were the fraction of MWCNT related to the total weight of the nanocomposite was only 16% wt., it can be observed that the excess of TiO_2 precursor results

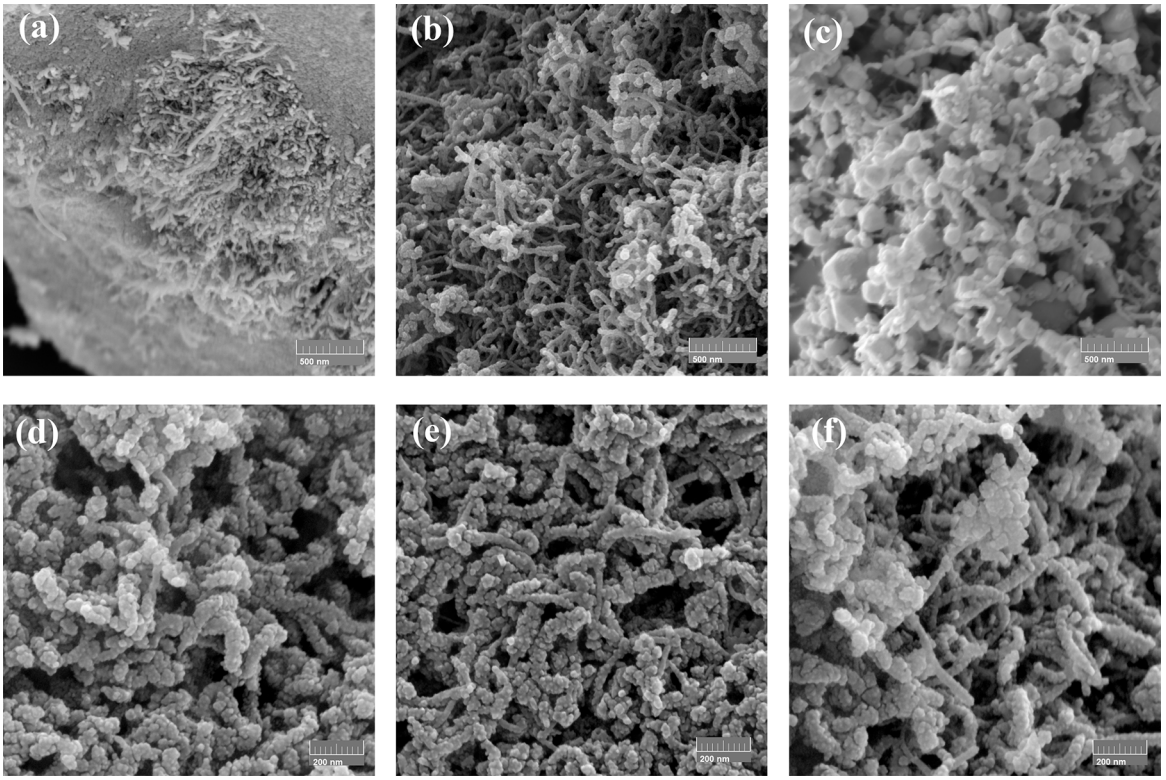

Figure 4. TiO_2 coated MWCNT obtained using 28 %wt. of MWCNT and a TTIP:H_2O molar ratio of: (a) 1:60, (b) 1:220, (c) 1:340. Coatings obtained with a fixed molar ratio of 1:220 with different MWCNTs to TiO_2 weight ratios: (d) 16% wt. and (e) 23% wt. In (f) a higher magnification of (b) is shown, for comparison purpose.

in a thicker deposit layer. Furthermore, as the nanotubes are completely coated, few isolated TiO_2 particles are also formed. Increasing the proportion of MWCNT to 23 wt.% (see Figure 4(e)), it seems that the TTIP was totally consumed to form a thick layer of TiO_2 over the nanotubes surface, and no isolated TiO_2 particles are formed. When the proportion of MWCNT was increased to 28 wt.%, the TiO_2 layer formed is very thin, see Figures 4(b) and (f) .

In order to assess the thermal stability of the TiO_2-coated MWCNT in air, thermogravimetric analyses in oxidizing atmosphere were performed in samples coated using the best coating condition: 1:220 TTIP:H_2O molar ratio and a MWCNT proportion of 23%wt., calcined at 500 and 1000ºC. For comparison purpose, results from uncoated MWCNT are also presented, although this comparison is not straight. From the total mass of calcined samples, only 23% corresponds to the MWCNT, the rest correspond to TiO_2. In the Figure 5(a), it is observed that the critical temperature in terms of mass loss due to the oxidation of nanotubes is around 500 to 600ºC. This is easily observed from the derivative thermogravimetry curve (DTG) shown in the Figure 5 (b). In order to be sure that there was no carbon oxidation during calcination and that mass losses during TGA analysis of calcined samples were related to carbon oxidation and not to volatiles usually present after sol-gel synthesis, some experiments involving calcination were repeated in the TGA equipment, under inert argon atmosphere. Such experiments simulated the calcination conditions, and a typical TGA curve obtained is shown as an insert in Figure 5(a). It can be observed from this figure that during calcination, about 10% of mass is lost, which can be related to volatiles. Consequently, it can be assumed that in calcined samples, the nanotubes are preserved. It can also be assumed that during the subsequent TGA analysis of calcined samples, under O_2 atmosphere, the mass losses are related exclusively to carbon oxidation.

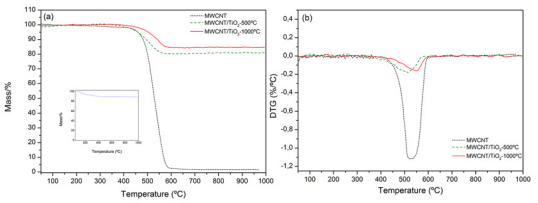

Figure 5.. Thermogravimetric analysis (a) and DTG (b) of MWCNT and TiO_2-coated MWCNT, calcined at 500 and 1000°C. The inset in (a) is TGA curve of MWCNT/TiO_2 performed in argon up to 1000ºC just before running the TGA analysis in an oxidizing atmosphere, for the TiO_2-coated MWCNT sample calcined at 1000ºC.

Table 2. Carbon content in TiO_2-coated MWCNT composites.

Initial MWCNT %wt.[1]	Calcination Temp. (°C)	TGA %wt. loss[2]. (%wt[1]/%wt[2])
23	500	19.7 (1.17)
23	1000	15.7 (1.46)

Notes: [1] MWCNT estimated from mass balance of the precursors;

[2] MWCNT lost during TGA analysis in O_2 atmosphere.

From the TGA analyzes of the TiO_2-coated MWCNT samples, it is possible to obtain the final mass of MWCNT and TiO_2 separately. It can be done supposing that the mass loss in O_2 atmosphere correspond to the mass of exposed (uncoated) carbon nanotubes that are burned out, while the mass of the stable TiO_2 remains unchanged. However, Figure 5 (a) shows that for samples having the same weight of MWCNT (23%), the mass loss changes, depending on the calcination temperature. For samples calcined at 500ºC, the lost mass that can be related to carbon nanotubes was 19.7% from the initial 23.0%, while for samples calcined at 1000ºC, this loss was 15.7%. In other words, 85.6% of MWCNT present in samples calcined at 500ºC were lost during heating while in samples calcined at 1000ºC, this lost decreased to 68.3%. Table 2 resumes the potential of protection that the TiO_2 layer confers to the MWCNT. Other important effect observed from the DTG curves in Figure 5 (b) is that the thermal stability of the MWCNTs was improved as the calcination temperature increased. The oxidation peak of the sample calcined at 500ºC occurs at a temperature of 522ºC, while for the sample calcined at 1000ºC this peak temperature increases by 30ºC.

Assuming that most of the MWCNT are covered by a thin TiO_2 layer, as observed in Figure 4 (e), and that during the calcination in inert argon atmosphere no carbon loss occurs (as it can be seen in inset of Figure 5 (a)), the overall results show that the TiO_2 layer shields the MWCNT protecting them from high temperature oxidation, at least partially. The data presented in Table 2 enables to quantitatively compare the protection level of the TiO_2 coating for different calcination temperatures. It is possible to note that the protection level expressed by the ratio between initial weight and weight loss, increases from around 1.17 to 1.46, when comparing the sample calcined at 500ºC with the sample calcined at 1000ºC. Consequently, this protection is more effective in samples calcined at 1000ºC. As the TiO_2 coating layer structure changes from porous Anatase to Rutile, as the calcination temperature increases, this better protection can be attributed to the denser and more stable Rutile phase. A denser coating reduces the paths available for oxygen to penetrate and interact with the MWCNT surface, increasing the time for diffusion and conferring a better protection against thermal oxidation. These results create new possibilities to produce MWCNT reinforced MMC by conventional and well established processing routes, reducing the risk of nanotubes damages caused by their exposition to high temperature cycles. Furthermore, the nanotubes dispersion and wettability in metal matrices can also be improved, enabling an overall improvement on the mechanical properties of the composites.

4. Conclusions

TiO_2 coated MWCNT hybrid materials have been successfully obtained by sol-gel technique, using titanium isopropoxide as a precursor. The best conditions were a molar ratio TTIP:H_2O of 1:220 and a mass proportion of 23% of MWCNT related to the total mass of TiO_2-coated MWCNT.

The increase in the I_D/I_G ratio obtained from Raman Spectroscopy confirm that the previous functionalization step was successful, as it introduces surface functional groups on the MWCNT surface that are necessary to the anchoring of the TiO_2 layer. X-Ray diffraction and Raman Spectroscopy shows that the TiO_2 layer crystallizes in the Anatase phase when calcined at 500ºC, and in the Rutile phase when calcined at 1000ºC. A small amount of Anatase still remains after calcination at this higher temperature.

Thermogravimetric analysis confirms that the TiO_2 coating layer confers a protection to the MWCNT in terms of high temperature oxidation. This protection is more effective as the layer is in the form of a dense and more stable rutile phase, obtained after inert gas calcination at 1000ºC.

5. Acknowledgments

The authors are thankful to the Associated Laboratory for Sensors and Materials (LAS-INPE - Brazil), for the FEG-SEM images and Raman Spectroscopy analysis and to CNPq for the financial support (Process No. 443395/2014-4).

6. References

1. Robertson DH, Brenner DW, Mintmire JW. Energetics of nanoscale graphitic tubules. Phys Rev B. 1992;45(21):12592.

2. Yao N, Lordi V. Young's modulus of single-walled carbon nanotubes. J Appl Phys. 1998;84(4):1939-43.

3. Demczyk BG, Wang YM, Cumings J, Hetman M, Han W, Zettl A, et al. Direct mechanical measurement of the tensile strength and elastic modulus of multiwalled carbon nanotubes. Mater Sci Eng A. 2002;334(1):173-8.

4. Gohardani O, Elola MC, Elizetxea C. Potential and prospective implementation of carbon nanotubes on next generation aircraft and space vehicles: A review of current and expected applications in aerospace sciences. Prog Aerosp Sci. 2014;70:42-68.

5. Li CD, Wang XJ, Wu K, Liu WQ, Xiang SL, Ding C, et al. Distribution and integrity of carbon nanotubes in carbon nanotube/magnesium composites. J Alloys Compd. 2014;612:330-6.

6. Bakshi SR, Singh V, Seal S, Agarwal A. Aluminum composite reinforced with multiwalled carbon nanotubes from plasma spraying of spray dried powders. Surf Coatings Technol. 2009;203(10-11):1544-54.

7. Ci L, Ryu Z, Jin-Phillipp NY, Rühle M. Investigation of the interfacial reaction between multi-walled carbon nanotubes and aluminum. Acta Mater. 2006;54(20):5367-75.

8. Liao J, Tan M-J. Mixing of carbon nanotubes (CNTs) and aluminum powder for powder metallurgy use. Powder Technol. 2011;208(1):42-8.

9. Laha T, Kuchibhatla S, Seal S, Li W, Agarwal A. Interfacial phenomena in thermally sprayed multiwalled carbon nanotube reinforced aluminum nanocomposite. Acta Mater. 2007;55(3):1059-66.

10. Bakshi SR, Singh V, Balani K, McCartney DG, Seal S, Agarwal A. Carbon nanotube reinforced aluminum composite coating via cold spraying. Surf Coatings Technol. 2008;202(21):5162-9.

11. Travessa DN, Lieblich M. Dispersion of Carbon Nanotubes in AA6061 Aluminium Alloy Powder by the High Energy Ball Milling Process. Mater Sci Forum. 2014;802:90-5.

12. Hosseini SA, Ranjbar K, Dehmolaei R, Amirani AR. Fabrication of Al5083 surface composites reinforced by CNTs and cerium oxide nano particles via friction stir processing. J Alloys Compd. 2015;622:725-33.

13. Kim WJ, Lee SH. High-temperature deformation behavior of carbon nanotube (CNT)-reinforced aluminum composites and prediction of their high-temperature strength. Compos Part A Appl Sci Manuf. 2014;67:308-15.

14. Kim HH, Babu JSS, Kang CG. Fabrication of A356 aluminum alloy matrix composite with CNTs/Al2O3 hybrid reinforcements. Mater Sci Eng A. 2013;573:92-9.

15. Li Q, Yan H, Ye Y, Zhang J, Liu Z. Defect location of individual single-walled carbon nanotubes with a thermal oxidation strategy. J Phys Chem B. 2002;106(43):11085-8.

16. Wu J, Zhang H, Zhang Y, Wang X. Mechanical and thermal properties of carbon nanotube/aluminum composites consolidated by spark plasma sintering. Mater & Des. 2012;41(0):344-8.

17. Kwon H, Estili M, Takagi K, Miyazaki T, Kawasaki A. Combination of hot extrusion and spark plasma sintering for producing carbon nanotube reinforced aluminum matrix composites. Carbon N Y. 2009;47(3):570-7.

18. Liu ZY, Xiao BL, Wang WG, Ma ZY. Developing high-performance aluminum matrix composites with directionally aligned carbon nanotubes by combining friction stir processing and subsequent rolling. Carbon N Y. 2013;62:35-42.

19. Khorasani S, Heshmati-Manesh S, Abdizadeh H. Improvement of mechanical properties in aluminum/CNTs nanocomposites by addition of mechanically activated graphite. Compos Part A Appl Sci Manuf [Internet]. 2015;68:177-83. Available from: http://linkinghub.elsevier.com/retrieve/pii/S1359835X14003212

20. Laha T, Agarwal A, McKechnie T, Seal S. Synthesis and characterization of plasma spray formed carbon nanotube reinforced aluminum composite. Mater Sci Eng A. 2004;381(1-2):249-58.

21. Kang K, Bae G, Kim B, Lee C. Thermally activated reactions of multi-walled carbon nanotubes reinforced aluminum matrix composite during the thermal spray consolidation. Mater Chem Phys [Internet]. 2012;133(1):495-9. Available from: http://linkinghub.elsevier.com/retrieve/pii/S0254058412000958

22. Yan L, Tan Z, Ji G, Li Z, Fan G, Schryvers D, et al. A quantitative method to characterize the Al4C3-formed interfacial reaction: The case study of MWCNT/Al composites. Mater Charact. 2016;112:213-8.

23. Deng CF, Wang DZ, Zhang XX, Li AB. Processing and properties of carbon nanotubes reinforced aluminum composites. Mater Sci Eng A. 2007;444(1-2):138-45.

24. Park JK, Lucas JP. Moisture effect on SiCp/6061 Al MMC: Dissolution of interfacial Al4C3. Scr Mater. 1997;37(4):511-6.

25. Manivannan R, Daniel A, Srikanth I, Kumar A, Sarkar R, Ghoshal P, et al. Thermal Stability of Zirconia-coated Multiwalled Carbon Nanotubes. Def Sci J. 2010;60(3):337-42.

26. Inam F, Vo T, Kumara S. Improving oxidation resistance of carbon nanotube nano- composites for aerospace applications. In: 2nd International Conference on Advanced Composite Materials and Technologies for Aerospace Applications. Wrexham, UK; 2012. p. 1-6.

27. Jo I, Cho S, Kim H, Jung BM, Lee S-K, Lee S-B. Titanium dioxide coated carbon nanofibers as a promising reinforcement in aluminum matrix composites fabricated by liquid pressing process. Scr Mater. 2016;112:87-91.

28. Gao B, Chen GZ, Li Puma G. Carbon nanotubes/titanium dioxide (CNTs/TiO2) nanocomposites prepared by conventional and novel surfactant wrapping sol-gel methods exhibiting enhanced photocatalytic activity. Appl Catal B Environ. 2009;89(3-4):503-9.

29. Gao B, Peng C, Chen G, Lipuma G. Photo-electro-catalysis enhancement on carbon nanotubes/titanium dioxide (CNTs/TiO2) composite prepared by a novel surfactant wrapping sol-gel method. Appl Catal B Environ. 2008;85(1-2):17-23.

30. Yan J, Wu G, Guan N, Li L, Li Z, Cao X. Understanding the effect of surface/bulk defects on the photocatalytic activity of TiO2: anatase versus rutile. Phys Chem Chem Phys. 2013;15(26):10978-88.

31. Silva WM, Ribeiro H, Seara LM, Calado HDR, Ferlauto AS, Paniago RM, et al. Surface properties of oxidized and aminated multi-walled carbon nanotubes. J Braz Chem Soc. 2012;23(6):1078-86.

32. Yan X, Tay BK, Yang Y. Dispersing and functionalizing multiwalled carbon nanotubes in TiO2 sol. J Phys Chem B. 2006;110(51):25844-9.

33. Peining Z, Nair AS, Shengyuan Y, Ramakrishna S. TiO 2 - MWCNT rice grain-shaped nanocomposites : Synthesis , characterization and photocatalysis. Mater Res Bull [Internet]. 2011;46(4):588-95. Available from: http://dx.doi.org/10.1016/j.materresbull.2010.12.025

34. Eder D, Windle AH. Morphology control of CNT-TiO2 hybrid materials and rutile nanotubes. J Mater Chem. 2008;18(17):2036-43.

35. Wu C-H, Kuo C-Y, Chen S-T. Synergistic effects between TiO 2 and carbon nanotubes (CNTs) in a TiO 2 /CNTs system under visible light irradiation. Environ Technol. 2013;34(17):2513-9.

36. Gui MM, Chai S-P, Xu B-Q, Mohamed AR. Visible-light-driven MWCNT@TiO2 core-shell nanocomposites and the roles of MWCNTs on the surface chemistry, optical properties and reactivity in CO2 photoreduction. RSC Adv. 2014;4(46):24007.

37. Zhou W, Pan K, Qu Y, Sun F, Tian C, Ren Z, et al. Photodegradation of organic contamination in wastewaters by bonding TiO2/single-walled carbon nanotube composites with enhanced photocatalytic activity. Chemosphere. 2010;81(5):555-61.

38. Hamid SBA, Tan TL, Lai CW, Samsudin EM. Multiwalled carbon nanotube/TiO2 nanocomposite as a highly active photocatalyst for photodegradation of Reactive Black 5 dye. Chinese J Catal. 2014;35(12):2014-9.

39. Spurr RA, Myers H. Quantitative Analysis of Anatase-Rutile Mixtures with an X-Ray Diffractometer. Anal Chem. 1957;29(5):760-2.

40. Mardare D, Tasca M, Delibas M, Rusu GI. On the structural properties and optical transmittance of TiO2 r.f. sputtered thin films. Appl Surf Sci. 2000;156(1):200-6.

41. Mali SS, Betty CA., Bhosale PN, Patil PS. Synthesis, Characterization of Hydrothermally Grown MWCNT-TiO2 Photoelectrodes and Their Visible Light Absorption Properties. ECS J Solid State Sci Technol. 2012;1(2):M15-23.

42. Stobinski L, Lesiak B, Kövér L, Tóth J, Biniak S, Trykowski G, et al. Multiwall carbon nanotubes purification and oxidation by nitric acid studied by the FTIR and electron spectroscopy methods. J Alloys Compd. 2010;501(1):77-84.

43. White CM, Banks R, Hamerton I, Watts JF. Characterisation of commercially CVD grown multi-walled carbon nanotubes for paint applications. Vol. 90, Progress in Organic Coatings. 2016. p. 44-53.